Suppressing Effects of Ag Wetting Layer on Surface Conduction of Er Silicide/Si(001) Nanocontacts *

Qing Han(韩青)[1,2], Qun Cai(蔡群)[1,2**]

[1] *State Key Laboratory of Surface Physics, and Department of Physics, Fudan University, Shanghai 200433*

[2] *Collaborative Innovation Center of Advanced Microstructures, Nanjing 210093*

(Received 3 April 2018)

Current-voltage electrical characteristics of Er silicide/Si(001) nanocontacts are measured in situ in a scanning tunneling microscopy system. Introduced as a new technique to suppress surface leakage conduction on Si(001), a silver wetting layer is evaporated onto the substrate surface kept at room temperature with $ErSi_2$ nanoislands already existing. The effects of the silver layer on the current-voltage characteristics of nanocontacts are discussed. Our experimental results reveal that the silver layer at coverage of 0.4–0.7 monolayer can suppress effectively the current contribution from the surface conduction path. After the surface leakage path of nanocontacts is obstructed, the ideality factor and the Schottky barrier height are determined using the thermionic emission theory, about 2 and 0.5 eV, respectively. The approach adopted here could shed light on the intrinsic transport properties of metal-semiconductor nanocontacts.

PACS: 73.63.Rt, 68.37.Ef, 68.35.−p, 73.25.+i   DOI: 10.1088/0256-307X/35/8/087301

Metal-semiconductor (MS) contact is an essential part of semiconductor electronic devices, the dimensional shrinkage of devices to the nanoscale produces ever-increasing requirements on the knowledge of the electrical transport properties across MS interfaces.[1,2] In the past ten years, MS nanocontacts have drawn tremendous research interests.[3−6] These nanocontacts embrace many MS interfaces with different space configurations, and some characteristic behaviors are observed in their electrical transports, such as highly large current density and its size dependence.[3,6,7] In addition to the thermionic emission theory, surface recombination-generation effect of minority carriers and tunneling effect have been proposed till now to explain the abnormal transport properties of the nanocontacts.[8,9] Metal silicide nanostructure/Si interface is a perfect nanocontact system, its contact area and interfacial atomic structure can be reliably regulated, as well as the shape of the silicide nanostructure.[3,5,7,9] In the electrical transports of these nanocontacts self-assembled on Si substrates, surface conduction was revealed to play a more dominant role than that through the contact interface.[10−12] This surface leakage current has to be eliminated, to gain an insight into the inherent properties of electrical transport through the nanocontact. Oxygen and ammonia adsorptions were utilized in the previous works to suppress the surface conduction path of the nanocontacts on Si substrates,[10,12] which usually affected the surface of silicide nanostructure and increased the contact resistance between the probing tip and nanostructure. More effects should be devoted to optimize the performance of nanocontacts and to disclose their intrinsic electrical transport properties. In literature, it was demonstrated that a wetting layer of lead on Si substrates can result in a conductive surface, while the Ag layer makes the surface insulating.[13] Therefore, we believe that a right metal layer can be employed to obstruct the surface leakage conduction of the nanocontacts formed between metal silicide nanostructures and Si.

In this work, a novel technique is introduced to restrain the surface conduction path of the nanocontacts on Si(001). We evaporate submonolayer Ag onto the Si(001) substrate kept at room temperature, with Er silicide nanoislands already existing. The experimental results show that surface leakage current can be suppressed effectively at some optimal Ag coverages. After the sample surfaces are insulated by the Ag wetting layer, the ideality factor n in the thermionic emission equation can be determined, as well as the Schottky barrier height. Their relationships with the interface area of $ErSi_2$ nanoislands will also be discussed.

All experiments were carried out in an Omicron ultrahigh vacuum scanning tunneling microscopy (STM) system, with a base pressure of less than 1.0×10^{-10} mbar. The Si(001) substrate with a resistivity of 4–8 Ω·cm was degassed at 600℃ overnight, and then was heated above 1200℃ to obtain a clean Si(001)-(2×1) surface. $ErSi_2$ nanoislands with tetragonal $ThSi_2$-type structure were self-organized on the Si substrate after 0.5 monolayer (ML) Er was deposited onto the Si(001) kept at room temperature and then the sample was annealed at 750℃ for 10 min.[14] Ag was subsequently evaporated onto the sample with the nanoislands at room temperature, from a Mo crucible

*Supported by the National Natural Science Foundation of China under Grant No 11374058.

**Corresponding author. Email: qcai@fudan.edu.cn

heated by an electron beam, and afterward this sample was transferred into the STM chamber before/after annealing for observations and measurements. The deposition rate of Ag was monitored by a quartz-crystal microbalance and was also calibrated using the STM images. The sample annealing temperature was measured using an infrared pyrometer with an uncertainty of ±20 K. The STM tips were fabricated by electrochemically etching the polycrystalline W wires, and they were heated *in situ* using the electron beam to remove oxides and contaminations. All STM topological images were obtained at room temperature, with the bias voltage of $\pm(0.8-2.0)$ V and the tunneling current of 0.15–0.30 nA. The current-voltage (I–V) characteristics of the nanocontacts between $ErSi_2$ nanoislands and Si(001) were measured by penetrating the tip directly into the silicide nanoislands with the feedback loop switched off and then ramping the sample bias.[15] The Er silicide nanoislands in the shape of a truncated pyramid (as shown in the inset of Fig. 1) have the base area in the range of 400–18000 nm^2, with the heights in the range of 7–10 nm. The geometry features of nanoislands, such as the interface area, were acquired simply using the commercial SPIP analysis software.

To obtain a reliable electrical contact between the STM tip and silicide nanoisland, the dependence of current I on the penetration depth Δz was investigated before the I–V measurements with/without the Ag layer.[15] Here Δz is the displacement of the STM tip toward the nanoisland surface, and the zero point of Δz is determined by the STM feedback condition. Figure 1 displays a typical relationship between I and Δz at a constant bias voltage. No discernible difference in I–Δz curves is observed for the samples with and without the Ag layer. It is shown that the current saturates at $\Delta z > 0.6$ nm, which can be regarded as the critical depth of good contact. The I–V curves in the following were all obtained at Δz of 1.2 nm, and for each curve 5–7 measurements were taken with good reproducibility.

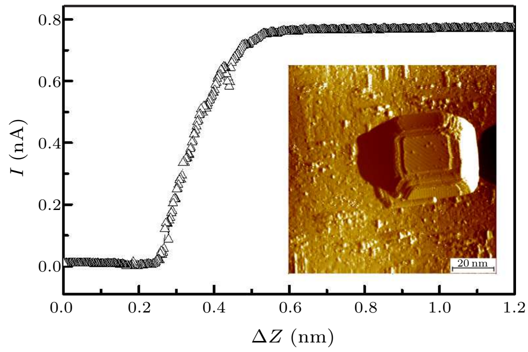

Fig. 1. The dependence of current I on the penetration depth. Here Δz is obtained under the STM feedback condition (2.0 V, 0.2 nA). The inset shows the STM current image of a typical Er silicide nanoisland self-organized on the sample surface. Tunneling conditions: 2.0 V, 0.2 nA.

To know enough about the site dependence of the electrical transport properties measured on the top surface of Er silicide nanoislands, the I–V characteristics were acquired on the same nanoisland at various locations. Table 1 lists the currents measured at 0.5 V on two different nanoislands, with interface areas of 4800 nm^2 and 4740 nm^2, respectively. The corresponding coverage of the Ag wetting layer is 0.7 ML. The currents from the 4800 nm^2 nanoisland were obtained at five different sites, while the data from the 4740 nm^2 nanoisland were measured twice at two different sites, respectively. The data listed in Table 1 imply that the measured currents are independent of the tip sites on the top surface of the same nanoisland, and a stable contact is well constructed between the STM tip and the silicide nanoisland.

Table 1. The current data obtained at 0.5 V on two different nanoislands.

Area (nm^2)	4800					4740			
Current (nA)	7.92	7.92	7.99	8.02	7.93	8.68	8.74	8.76	8.7

To clarify the effects of the Ag wetting layer on the electrical characteristics of Er silicide/Si(001) nanocontacts, the experimental procedures of Ag evaporation should be given in careful consideration. Figure 2 shows the typical STM images obtained on the Si(001) substrate, after the Ag layer evaporated onto the substrate is kept at room temperature and then annealed at an elevated temperature. Ag induced (2×3) and $c(6\times2)$ reconstructions can be clearly seen on the sample surface, consistent with the previous results.[16,17] In Fig. 2(a), 0.2 ML Ag on Si(001) mainly brings about black wires perpendicular to the Si dimer rows after 550℃ annealing, very similar to the missing Si dimer defects. The arrow in the figure denotes the direction of Ag-induced black wires. When Ag coverage is increased to 0.8 ML, as shown in Fig. 2(b), a mixture of (2×3) and $c(6\times2)$ reconstructions can be found to cover the surface. It is established that these Ag-decorated Si(001) surfaces show semiconducting electrical properties.[18–20] With Ag coverage more than 1.0 ML, three-dimensional metallic Ag islands will appear on the surface, surrounded by the reconstructed surface.[21]

Due to the formation of Ag-induced surface reconstructions on Si(001), Er silicide nanoislands were produced on the clean Si substrate first, to avoid the possible influence of the Ag layer on the island growth behavior and the interface characteristics. The I–V

curves were measured subsequently for the $ErSi_2$/Si nanocontacts after Ag was evaporated onto the identical sample with different coverages. The typical I–V curves are shown in Fig. 3, which are acquired separately on the nanoislands with different contact areas. The corresponding Ag coverages are indicated in the figures, as well as the interface areas of the nanocontacts. Here the positive bias corresponds to the forward bias of a Schottky diode. It can be seen that without the Ag layer the current increases rapidly with forward bias after a turn-on voltage of ~0.1 V, making the I–V curve exhibit in an exponential form. At the reverse bias, the current is found to display evidently a linear tendency with the bias. These electrical transport behaviors were observed in our previous works and were attributed to the effects of surface-state conduction and surface barrier conduction.[10,15]

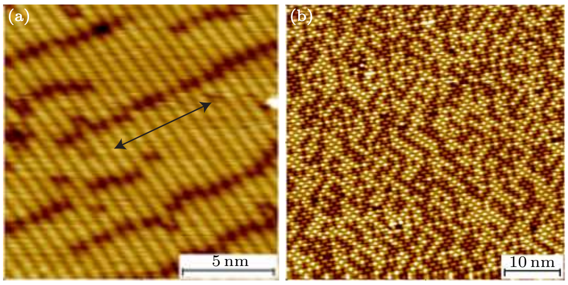

Fig. 2. Two filled-state STM images obtained on the Si(001) surface after (a) 0.2 ML, and (b) 0.8 ML Ag evaporated on the clean substrate at room temperature and then annealed for 5 min at (a) 550°C, and (b) 720°C. The bias voltages are −1.1 V and −2.0 V, respectively.

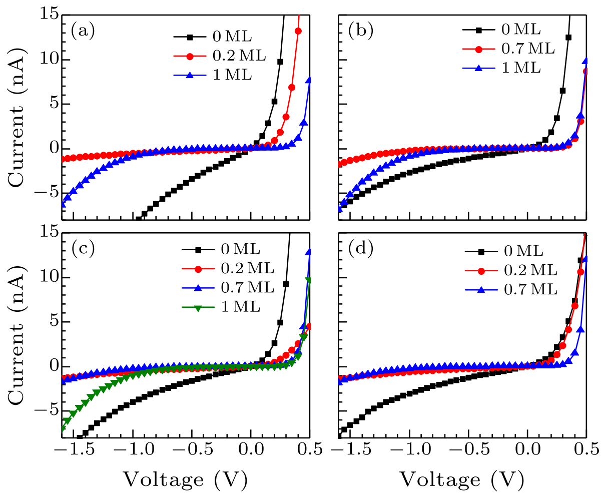

Fig. 3. The I–V characteristic curves obtained on the nanoislands at different Ag coverages, with the contact areas of (a) 4500 nm^2, (b) 4800 nm^2, (c) 5400 nm^2, and (d) 7000 nm^2, respectively.

The I–V curves in Fig. 3 also exhibit distinctly the dependence on Ag coverage, although the curves are obtained separately on four nanocontacts. It is manifested that at forward bias the existence of the Ag layer always makes the turn-on voltage increase to 0.2 V, and a high coverage can cause the turn-on voltage to raise even more. The I–V characteristic curve at reverse bias indicates definitely that the Ag layer can bring about a significantly enhanced rectifying feature. For the 0.2 ML Ag layer the breakdown voltage for the reverse bias is recognized as 0.9–1.0 V, and for 0.7 ML this breakdown voltage seems to increase slightly more. It is also noticed that with 0.2 ML Ag the I–V curves at reverse bias exhibit a nearly linear relationship with the bias, despite the small slope of the curves. When the coverage increases to 1.0 ML, the reverse-bias breakdown voltage usually lessens to about 0.8 V.

Our experimental results reveal that the Ag layer can eliminate the surface current from the I–V curves of the $ErSi_2$/Si(001) nanocontacts. Wang *et al.* have shown that the poor conductivity of the Ag wetting layer on the Si(111) substrate can make the surface insulating.[13] On Si(001) surface, the small difference in electronegativity results in the covalent bonding formed between Ag and Si.[20] It should be pointed out that annealing at elevated temperature is indispensable for the growth of Ag $c(6 \times 2)$ and (2×3) reconstructions on Si(001).[17] Finally several surface-state bands will be found within the bulk bandgap for these Ag-decorated Si(001) surfaces, with binding energies >0.7 eV.[18,19] As demonstrated in our experiments, the Ag layer has to be evaporated onto Si(001) at room temperature to avoid the impact to the existing nanocontacts. Er-induced reconstructions already exist on the surface regions among $ErSi_2$ nanoislands before Ag deposition, and Er dimers have been shown to partially substitute for Si dimers on Si(001).[22] Our previous investigations verified that this reconstructed surface could provide a remarkable contribution of surface current to the I–V curves.[15] In this work, the obtained I–V curves indicate that the Ag layer can make the surface electrical conduction path cease to be in effect on the samples of $ErSi_2$ nanoislands/Si(001). Ag atoms are known not to diffuse into the Si substrate with a low solid solubility, and the saturation coverage of Ag (2×3) and $c(6 \times 2)$ reconstructions is 0.50–0.67 ML.[17] It is reasonable to assume that the evaporated Ag atoms passivate the sample surface due to the formation of Ag-Si bonding, therefore suppress the surface electrical current.[20] With increasing the coverage from 0.2 to 0.7 ML, more formations of Ag–Si bonding can be achieved on the surface, finally improving the suppressing efficiency. When Ag coverage increases beyond its saturation value on Si(001) to 1.0 ML, Ag–Ag bonding will appear presumably on the sample surface, reducing the breakdown voltage of the I–V curves at reverse bias.

To ascertain the effects of the Ag wetting layer on the surface conduction of $ErSi_2$/Si(001) nanocontacts, the current density-voltage (J–V) curves were measured on the nanoislands with various interface areas after Ag evaporated on the sample surfaces at different sub-monolayer coverages. As shown in Fig. 4, these J–V curves are exhibited with Ag coverages of 0.2 ML, 0.4 ML, and 0.7 ML, respectively, where coverage dependence of nanocontact transport properties can be examined clearly. For the samples covered with 0.2 ML Ag, the current density bears a linear correlation with the reverse bias, implying that the contribution from the surface conduction path has not been entirely removed. For 0.4 ML and 0.7 ML Ag, the J–V curves show much better rectifying behavior. The slopes of the backward J–V curves for the nanocontacts covered with 0.2 ML Ag are found in one order of magnitude larger than those for the nanocontacts with 0.4 and 0.7 ML Ag.

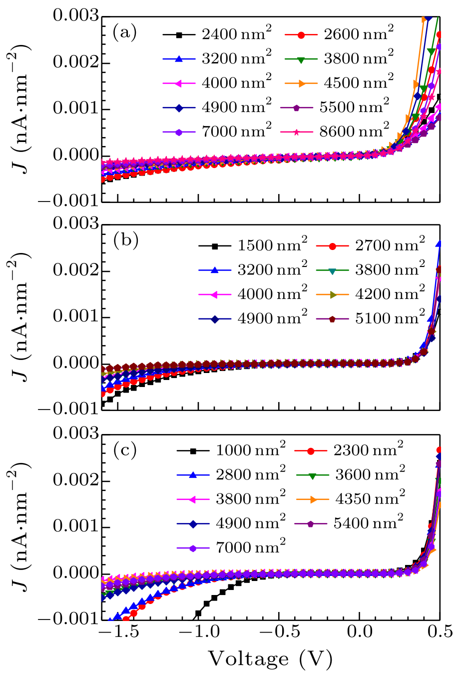

Fig. 4. The J–V curves obtained on the nanoislands with various interface areas after (a) 0.2 ML, (b) 0.4 ML, and (c) 0.7 ML Ag evaporated onto the sample surface.

The J–V characteristic curves shown in Fig. 4 can be fitted using the thermionic emission theory described by[23]

$$I = AA^{**}T^2 \exp(-q\Phi_{\rm eff}/kT)[\exp(qV/nkT) - 1],$$

where the current density $J = I/A$, A is the contact area, A^{**} is the effective Richardson constant, T is the absolute temperature, q is the elementary electric charge, k is the Boltzmann constant, $\Phi_{\rm eff}$ is the effective Schottky barrier height (SBH), and n is the ideality factor. For conventional Schottky diodes, n is equal or close to 1. As shown in Fig. 5, the results of n and $\Phi_{\rm eff}$ determined from the J–V curves in Fig. 4 are plotted as a function of the contact area. It is observed that for 0.2 ML Ag the values of n are much larger than 1, ranging from 3 to 7, and the SBHs are found to range from 0.3 to 0.4 eV. We attribute the large values of the n factor with high dispersion to the incomplete suppressing effect of 0.2 ML Ag on surface conduction. The residual surface currents for the nanocontacts with various areas make the J–V curves at low bias very different from those described by the thermionic emission equation, bringing about the large and fluctuant values of ideality factor lastly. The values of n factor for 0 and 1.0 ML Ag also show the same dependence on contact area. For 0.4 and 0.7 ML Ag, n shows the reduced value, varying from 2 to 3, and the SBH increases to about 0.5 eV. It is also noteworthy that n has a large value for the nanocontacts with small interface area, probably a result of the reduced barrier width to enhance the tunneling of carriers. At the same time, the SBH seems to increase with the contact area. These experimental results demonstrate further that the Ag layer at coverage of 0.4–0.7 ML can suppress the surface electrical conduction effectively for the $ErSi_2$/Si(001) nanocontacts. Without surface conduction, the fundamental features of electrical transport properties can be investigated thoroughly for MS nanocontacts. For the nanocontacts less than 2000 nm^2, more experimental researches should be performed to explore whether or not the tunneling effect causes the large ideality factor.

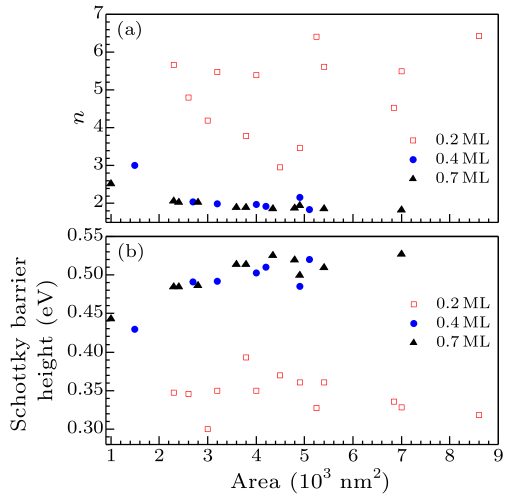

Fig. 5. The ideality factor n and the effective SBH are plotted as a function of contact area for different coverages of the Ag wetting layer.

In summary, the electrical transport characteristics of Er silicide/Si(001) nanocontacts have been studied using I–V measurements with an STM tip touching directly on the top surface of $ErSi_2$ nanoislands. A new approach to suppress surface leakage conduction is proposed, in which submonolayer Ag is evaporated onto the Si(001) surface kept at room temperature with $ErSi_2$ nanoislands already existing. The STM measurements show that the 0.4–0.7 ML

Ag layer can eliminate effectively the current contribution from the surface conduction path for the $ErSi_2$/Si(001) nanocontacts. This approach will make it possible to reveal thoroughly the intrinsic transport properties of $ErSi_2$/Si(001) nanocontacts.

References

[1] Léonard F and Talin A A 2011 *Nat. Nanotechnol.* **6** 773
[2] Requist R, Baruselli P P, Smogunov A, Fabrizio M, Modesti S and Tosatti E 2016 *Nat. Nanotechnol.* **11** 499
[3] Kubo O, Shingaya Y, Aono M and Nakayama T 2006 *Appl. Phys. Lett.* **88** 233117
[4] Vitali L, Levita G, Ohmann R, Comisso A, De Vita A and Kern K 2010 *Nat. Mater.* **9** 320
[5] Liu X Y, Zou Z Q, Sun L M and Li X 2013 *Appl. Phys. Lett.* **103** 043116
[6] Lord A M, Maffeis T G, Kryvchenkova O, Cobley R J, Kalna K, Kepaptsoglou D M, Ramasse Q M, Walton A S, Ward M B, Koble J and Wilks S P 2015 *Nano Lett.* **15** 4248
[7] Liu X Y and Zou Z Q 2015 *Nanotechnology* **26** 195704
[8] Lee S Y and Lee S K 2007 *Nanotechnology* **18** 495701
[9] Hao L and Bennett P A 2009 *Nanotechnology* **20** 355201
[10] Song J Q, Ding T and Cai Q 2010 *Appl. Phys. Lett.* **96** 203113
[11] Zou Z Q, Liu X Y, Sun L M and Li X 2014 *Appl. Phys. Lett.* **105** 231606
[12] Dupont-Ferrier E, Mallet P, Magaud L and Veuillen J Y 2007 *Phys. Rev.* B **75** 205315
[13] Wang K, Zhang X, Loy M M T and Xiao X 2008 *Surf. Sci.* **602** 1217
[14] Ding T, Wu Y, Song J, Li J, Huang H, Zou J and Cai Q 2011 *Nanotechnology* **22** 245707
[15] Song J Q, Ding T, Li J and Cai Q 2010 *Surf. Sci.* **604** 361
[16] Lin X F, Wan K J and Nogami J 1994 *Phys. Rev.* B **49** 7385
[17] Takeuchi O, Kageshima M, Sakama H and Kawazu A 2001 *Jpn. J. Appl. Phys.* **40** 4414
[18] Yeom H W, Matsuda I, Tono K and Ohta T 1998 *Phys. Rev.* B **57** 3949
[19] Matsuda I, Yeom H W, Tono K and Ohta T 1999 *Phys. Rev.* B **59** 15784
[20] Matsuda I, Yeom H W, Tono K and Ohta T 1999 *Surf. Sci.* **438** 231
[21] Lin X F, Wan K J and Nogami J 1993 *Phys. Rev.* B **47** 10947
[22] Zhu Y, Zhou W, Wang S H, Ji T, Hou X Y and Cai Q 2006 *J. Appl. Phys.* **100** 114312
[23] Sze S M 1981 *Phys. Semiconductor Devices* 2nd edn (New York: Wiley)